Adatom-dependent diffusion mechanisms on a Ag/Si(111)$\sqrt{3}\times\sqrt{3}$ surface

Sukmin Jeong* and Hojin Jeong
Department of Physics and Research Institute of Physics and Chemistry, Chonbuk National University, Jeonju 561-756, Korea
(Received 1 February 2010; revised manuscript received 28 April 2010; published 25 May 2010)

We present first-principles calculations for the diffusion of monovalent alkali and noble metal adatoms on a Ag/Si(111)$\sqrt{3}\times\sqrt{3}$ ($\sqrt{3}$-Ag) surface, a two-dimensional (2D) electron gas system tunable via the electron doping of adatoms in 2D adatom gas. In this system, a Ag adatom diffuses over the surface through an exchange mechanism in which the adatom and the substrate Ag atoms exchange repeatedly in each diffusion step. The resulting calculated diffusion barrier is only 0.22 eV. Other adatoms (Au, Cu, Li, and Na) are incorporated into the substrate via exchange with a Ag atom followed by the Ag atom diffusion on the surface. The calculated site-projected densities of states show that the adatom and the substrate Ag atoms have a clear difference in their empty states, which can be used to verify an exchanged configuration for the heterogeneous adatoms. On the other hand, a K adatom with a large atomic radius favors a direct diffusion with a barrier of 0.12 eV. Depending on the adatoms on the $\sqrt{3}$-Ag surface, the various diffusion mechanisms can be traced to the tensile surface stress due to the Ag layer expansion and the surface chemistry related with the heterogeneous (Ag and Si) overlayer, leading to an unusual microscopic mechanism of 2D adatom-gas formation.

DOI: 10.1103/PhysRevB.81.195429 PACS number(s): 68.35.Fx, 68.43.Fg, 68.43.Jk, 68.55.Ln

I. INTRODUCTION

The Ag-induced $\sqrt{3}\times\sqrt{3}$ layer on Si(111) ($\sqrt{3}$-Ag hereafter) has been a model system of a surface two-dimensional electron gas (2DEG) with a well-defined 2D metallic band.[1–18] A novel feature of this system is that the metallic electron density is freely tunable by electron doping from extra metallic adatoms such as noble (Au and Ag) and alkali (Cs, K, Na, and Li) metals. Although the tuned 2D electron band and the localized electron state of dopants have been clearly observed by angle-resolved photoemission (ARP) spectroscopy,[2–4] the adatoms themselves could not be probed directly, in particular, by scanning tunneling microscopy (STM), presumably due to their high mobility. This high mobility is thought to drive the system into a 2D atomic gas (2DAG) state,[3,5] which, depending on the density, freezes into a random or ordered adatom array at low temperatures. Only at low temperature could STM observe the characteristic images of a single unit of dopants, which was interpreted as being due to a specific cluster of adatoms.[13–16] Thus, this surface seems to pose a unique nontrivial 2DEG system coupled with a 2DAG; the dopants (doping) can either be in a gas (dynamic) or solid (static) state. Previous first-principles calculations[15,16] clarified the structures of adatom clusters and proposed a new structure model for the adatom-induced $\sqrt{21}\times\sqrt{21}$ surface, along with its electronic structure. However, no kinematical information on the adatoms is yet available to address their diffusion mechanism leading to the 2DAG behavior.

In this paper, we explore the diffusion of monovalent noble and alkali metal adatoms on a $\sqrt{3}$-Ag substrate using first-principles total-energy calculations. For a homogeneous adsorption, a Ag adatom migrates on the surface through repeated exchanges of the adatom and the substrate Ag atoms. In the case of heterogeneous adsorption, Cu, Au, Li, and Na adatoms favor substitution with a substrate Ag atom, implying that Ag atoms then diffuse. On the contrary, a K adatom diffuses by direct hopping between metastable sites. In all cases, the corresponding energy barriers are less than or comparable to 0.2 eV, consistent with the 2DAG behavior of the adatoms on $\sqrt{3}$-Ag. The structures formed by the adatom exchange for heterogeneous adatoms can be distinguished from the unexchanged structure by site-projected densities of states (DOSs), which produce different curves for the adatom and the substrate Ag atoms.

II. CALCULATION METHOD

Calculations are performed using the Vienna *ab initio* simulation package[19] which incorporates ultrasoft pseudopotentials[20] and the generalized gradient approximation of Perdew and Wang[21] for the exchange-correlation energy. The surface is simulated by a repeated slab model with a $4\sqrt{3}\times4\sqrt{3}$ lateral periodicity in which six Si layers and a 10 Å vacuum layer are included. We use a 13 Ry cut-off energy for the plane-wave basis and a 2×2 k-point mesh for the surface Brillouin zone sampling which produce well-converged results.[15,16,22] The pathways and activation energies for the adatom diffusion processes are calculated using the nudged elastic band method.[22–24]

III. RESULTS AND DISCUSSION

The $\sqrt{3}$-Ag surface has a unique structure with both Si and Ag atoms forming heterogeneous triangles on top of the bulk-terminated Si(111) layer, one that includes Si and the other two that include Ag adatoms. The Ag triangles undergo a structural phase transition at 150 K into an inequivalent triangle reconstruction[18] [Fig. 1(A)] in which the small Ag triangles appear bright and the large Ag triangles appear dark under STM.[15,16,18] The calculated sizes of larger and smaller triangles are 3.88 Å and 3.00 Å, respectively. Monovalent metal adatoms stably adsorb onto the centers of the substrate triangles, small Ag triangles (ST), large Ag triangles (LT), and Si triangles (SiT). Figures 1(B) and 1(D) show the equilibrium structures of a Ag adatom on the LT and ST sites,

 ©2010 The American Physical Society

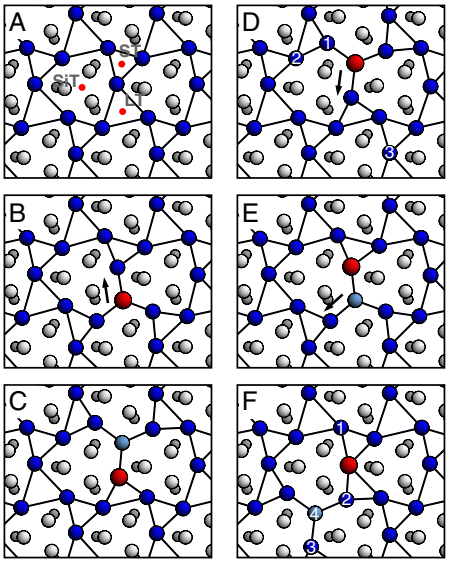

FIG. 1. (Color online) (A) Substrate structure and (B)–(F) various adsorption structures of a single Ag adatom. In A, the stable adsorption sites of ST, LT, and SiT are indicated. Large dark, small dark, and small white circles represent the Ag adatom, the substrate Ag atoms, and Si atoms forming triangles, respectively. The smaller circles denote the Si atoms in the deeper layers. In (B)–(F), the lightly shaded circles and arrows denote the moving atoms and their moving directions in diffusion processes (see the text), respectively.

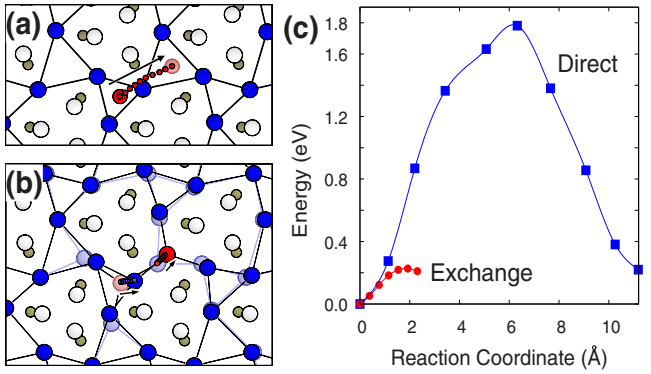

FIG. 2. (Color online) (a) Direct, (b) exchange diffusion of a Ag adatom, and (c) corresponding energy variations as a function of the reaction coordinate in the configuration space. In (b), lightly colored spheres represent the initial ST adsorption structure and darkly colored spheres represent the final LT structure. In (a) and (b), the intermediate positions of the adatom and an apex Ag atom are indicated by the smallest points.

respectively. As reported in a previous paper,[15] an adatom on the ST site induces significant structural changes in the substrate Ag layer. For other adatoms, with the exception of K with a large atomic radius, the top views of the equilibrium structures are nearly indistinguishable from those of the Ag atom. One of the major differences is the height of the adatom; noble metals immerse into the substrate Ag layer, while alkali metals with large atomic radii (Na and K) sit above the Ag layer (refer to Table II in Ref. 15).

Table I lists the relative energies for the metal adatoms on various sites. Among the various structures, the ST site is the most stable for Ag, Au, and Li while the LT site is the most stable for K. For Cu and Na, the ST and LT sites are energetically comparable. The SiT site is energetically comparable to the most stable LT site for K, but is the least stable for other adatoms. It is noted that for the heterogeneous adatoms of Au, Cu, and Na the exchanged structures, where the adatom occupies an apex of a substrate triangle with a Ag atom at the ST or LT site (Figs. 1(C) and 1(E) or Fig. 1(F)), are energetically more favorable than the unexchanged structures. On the other hand, all the exchanged structures of the K adatom have higher energies than LT or SiT structure.

Having established the adsorption structures, we next detail the atomistic processes for adatom diffusion on the $\sqrt{3}$-Ag surface. First, we consider the direct hopping of the Ag adatom from the ST site to the LT site, the nearest site with a local energy minimum, as shown in Fig. 2(a). The resulting energy variation along the diffusion pathway (relaxed fully and thus energy optimized) shows that the energy barrier is as large as 1.78 eV [Fig. 2(c)]. Assuming a typical prefactor value for Si of 10^9–10^{12} Hz, the attempting frequency from the ST site would be smaller than 10^{-20} s^{-1} at RT, i.e., practically immobile at or below RT along this pathway. This is in clear contradiction to the STM experiments.[3,5]

Another possible pathway is the exchange of an adatom and a neighboring substrate Ag atom at each diffusion step. Figure 2(b) displays such an exchange diffusion starting from the ST site to the nearest LT site. The adatom (large dark circle) pushes a neighboring Ag atom to constitute the apex of the small triangle with the pushed Ag atom (heavy red circle) at the center of the large triangle. The final structure is identical to the LT structure formed in the previously described direct hopping pathway. The Ag atom at the LT

TABLE I. Relative energies of metal adatoms for the various adsorption sites shown in Fig. 1. In G (not shown in Fig. 1), a Ag atom occupies an LT site neighboring the ST site of Fig. 1(F). The reference energy is the lowest energy for each adatom. All figure values are in electron volt.

Adatoms	B (LT)	C	D (ST)	E	F	G	(SiT)
Ag	0.22	0.00	0.00	0.22	0.00	0.22	1.35
Au	0.19	−0.08	0.00	0.15	−0.15	0.08	1.82
Cu	0.01	−0.07	0.00	−0.09	−0.06	0.12	1.23
Li	0.05	−0.01	0.00	0.18	0.10	0.24	0.47
Na	0.02	−0.12	0.00	−0.07	0.01	0.10	0.20
K	0.00	0.04	0.10	0.07	0.21	0.03	0.02

TABLE II. Energy barriers of metal adatoms for the direct diffusions between two metastable sites among ST, LT, and SiT. The barriers are measured for processes with the lower-energy site as the initial site. All figure values are in electron volt.

	ST-LT	LT-SiT	ST-SiT
Ag	1.78	1.13<	1.35<
Au	1.17	1.63<	1.82<
Cu	1.21	1.22<	1.23<
Li	0.83	0.54	0.71
Na	0.36	0.20	0.33
K	0.41	0.12	0.31

site, ejected from the small triangle, becomes a new diffusing species. In this way, the exchange repeats in each diffusion step. The calculated energy barrier for the ST→LT process decreases to 0.22 eV, which is comparable to that of Ag diffusion on a H-terminated Si(111) surface,[22] where adatom migration is very active. Assuming the same prefactor as above, we obtain attempting frequencies of 10^5–10^8 s^{-1} and 10^{-9}–10^{-6} s^{-1} for RT and 65 K, respectively. These frequencies are consistent with the 2DAG behavior observed by STM,[3] where no adatom is observable at RT, but many immobile bright features are evident at 65 K. The diffusion process through a SiT site is unlikely due to its high energy relative to ST or LT sites (Tables I and II), implying that the Si triangles function as diffusion blockades. This exchange diffusion process is unique with the pair of old and new diffusing Ag atoms below the substrate Ag layer. The quenching of diffusion at low temperature provides an explanation for the characteristic band splitting in ARP due to randomly distributed adatoms.[3] At RT, the rapidly moving adatoms generate averaging effects in the potential, resulting in the disappearance of band splitting.

The small diffusion barrier of a Ag adatom on the $\sqrt{3}$-Ag surface provides a high probability for the adatoms to form dimers, trimers, tetramers, or larger clusters. Indeed, a previous calculation[15] revealed that clustering is energetically favorable with binding energies for the two-, three-, and four-Ag clusters calculated to be 0.31 eV, 0.48 eV, and 0.11 eV, respectively.

The exchange diffusion mechanism is next applied to heterogeneous adatoms. For example, a Au adatom on the ST site [Fig. 1(D)] substitutes a neighboring Ag atom which then becomes a new adatom [light blue in Fig. 1(E)]. Consequently, the diffusion of Ag atoms takes place through the exchange mechanism as described previously (D→E→F). The energy barrier for D→E is roughly 0.15 eV, the energy difference between the D and E structures.[25] After the nearly zero-barrier stage of E→F, the diffusion species encounter a barrier of ~0.22 eV for F→G (because Ag is the diffusing species at this point, the diffusion barrier is similar to that of a Ag adatom in self-diffusion). As shown in Table I for Cu, Li, and Na, the diffusion barriers for the exchange processes from D through E and F to G are of similar magnitude to that of the Ag case. Therefore, the overall energy barriers of the exchange diffusion are ~0.2 eV for all the adatoms except for K. This exchange diffusion is favored over the direct

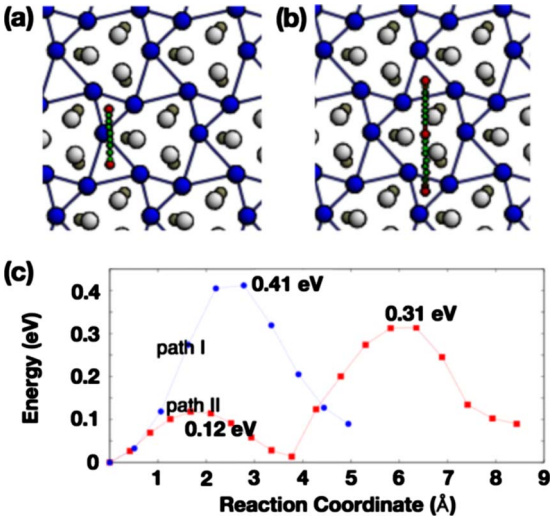

FIG. 3. (Color online) (a) Diffusion pathway from ST to LT (path I) and (b) from LT to SiT to ST (path II) for a K adatom. (c) Corresponding energy variations as a function of the reaction coordinate in the configuration space. In (a) and (b), the intermediate positions of the adatom are indicated by the smallest points.

diffusion because the energy barrier of the exchange diffusion is much lower than those of the direct diffusion, 0.36–1.78 eV (second column in Table II).

For K, unlike other adatoms, the exchange process is improbable since the exchanged structures of Figs. 1(C), 1(E), and 1(F) have higher energies than does the most stable LT structure (Table I). The energy barriers of the exchange process from the most stable LT site [Fig. 1(B)] to the exchanged structure [Fig. 1(C)] is only 0.04 eV. [It should be noted that the new adatom (light blue) occupies the ST site in the C structure, which is a low-energy structure of the Ag adatom.] In the next exchange step, the diffusing species (Ag atom) occupies a neighbor LT site with an energy increase to 0.30 eV [from Fig. 1(C)]. Thus the overall energy barrier for the exchange configuration is estimated to be 0.30 eV.

Figure 3 shows the diffusion pathways and the corresponding energy variations for the direct diffusion of the K adatom. The energy barriers for LT→ST (path I), LT→SiT (path II), and SiT→ST (path II) are 0.41 eV, 0.12 eV, and 0.31 eV, respectively. The most favorable pathway for direct diffusion is migration of K between the LT sites via the relatively stable SiT site with an energy barrier of 0.12 eV, which is much lower than the 0.30 eV energy barrier of the exchange process. Thus, these results indicate that, unlike for other adatoms, direct diffusion is favored for K.

The unique heterogeneous overlayer structure composed of Ag and Si triangles on $\sqrt{3}$-Ag provides interesting variations in the adatom diffusion mechanism depending on the kind of adatom. The lattice constant of Si along the [111] direction is 33% larger than that of Ag, implying that in principle 1.78 ML of Ag can be incorporated as an overlayer. But in reality only 1 ML of Ag saturates the Si surface, and hence the interatomic distances of Ag on the $\sqrt{3}$-Ag surface, 3.00–3.88 Å, are much longer than that of bulk Ag, 2.94 Å, i.e., the Ag overlayer of the $\sqrt{3}$-Ag surface is expanded compared to its bulk state. For the Ag adatom, the preference of

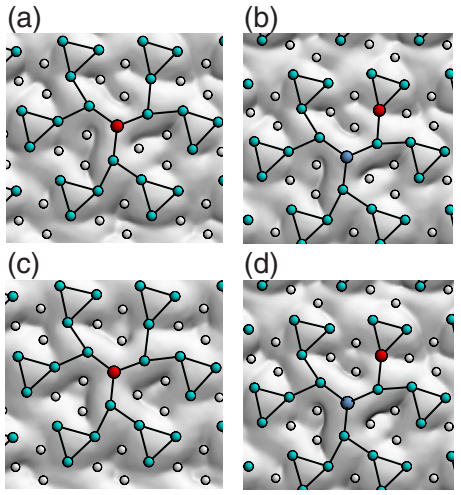

FIG. 4. (Color online) Simulated empty-state STM images of [(a) and (c)] the D structure and [(b) and (d)] the F structure in Fig. 1. (a) and (b) are for a Au adatom and (c) and (d) are for a Li adatom. In all the images, the biases are 1.0 V and the corresponding calculated equilibrium structures are superimposed. The STM images are calculated following the Tersoff-Hamann theory (Ref. 27) and represented by each isosurface (Ref. 28).

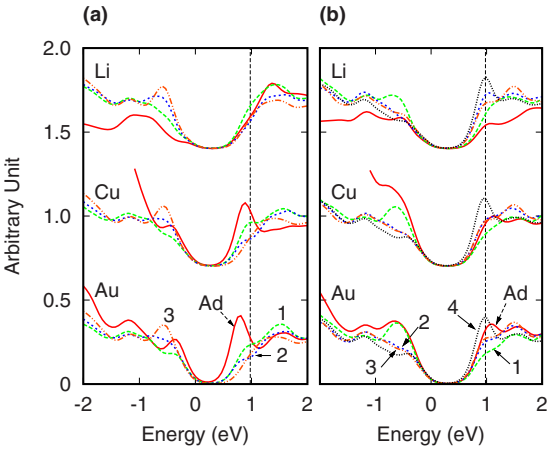

FIG. 5. (Color online) Site-projected density of states of (a) the D structure and (b) the F structure in Fig. 1 for Au, Cu, and Li adatoms. The numbered curves represent the DOSs related with the atoms numbered in Figs. 1(D) and 1(F). The dashed vertical lines indicated the position of the Ag peak on the ST site of the F structure. Reference energy is the Fermi energy of each structure.

exchange diffusion over direct diffusion can be understood in terms of the tensile stress on the expanded Ag regions. A similar mechanism has been invoked for the self- (exchange) diffusion on transition-metal surfaces.[26] The expanded Ag layer also enables other adatoms to occupy the exchanged site with relatively low-activation energies (Table I). After the exchange process, diffusion then takes place via Ag exchange since the original heterogeneous adatom is embedded in the substrate site. For the K adatom with $r_K = 1.56 r_{Ag}$, unlike smaller adatoms, the exchange process is endothermic. In addition to the surface stress, a chemical effect plays an important role in this adatom diffusion. While the SiT site is much less stable than other sites for noble metals, it is energetically comparable to other sites for alkali metals and is even close to the lowest-energy site for K. Thus, as previously mentioned, the Si triangles work as diffusion blockades for noble-metal adatoms. On the other hand, the K adatom migrates between the LT sites via the SiT site with an energy barrier of only 0.12 eV. Therefore, the tensile surface stress and the surface chemistry related to the heterogeneous overlayer are crucial in understanding adatom diffusion on the $\sqrt{3}$-Ag surface.

Heterogeneous adatoms on the $\sqrt{3}$-Ag surface substitute the substrate Ag atoms through the exchange process that embeds them into the Ag layer. The process provides a plausible way of forming an alloy layer with adatoms. This implies that the cluster features in STM images[3,13] could be due to Ag atoms and not due to the adsorbed foreign atoms because the atomic species, especially with the same valence, are not distinguishable in STM as confirmed in the simulated STM images shown in Fig. 4. The image of the unexchanged D structure with a Au adatom [Fig. 4(a)], in which the adatom, the neighboring (shrunken) LTs, and the next-neighboring STs look bright, resembles that of a Ag adatom (refer to Fig. 4 in Ref. 15). In addition, the unexchanged and the exchanged structures appear almost identical in their STM images [compare Figs. 4(a) and 4(b)]. This is true of other adatoms, Li [Figs. 4(c) and 4(d)] and Cu. However, a Na atom with a large atomic size is located ~1 Å above the Ag layer in the exchanged F structure, which implies that the adatoms could be distinguishable in STM measurements.

Although the exchange mechanism and its results proposed in the present papers are hardly observed, delicate differences in the electronic structures for different adatoms can be detected in scanning tunneling spectroscopy (STS) through dI/dV measurements. Figure 5 shows the site-projected DOSs for Au, Cu, and Li adatoms on the ST site [Fig. 1(D)] and the exchanged structure with Ag at the ST site [Fig. 1(F)]. Conspicuous peaks around 0.8–0.9 eV are seen for Au and Cu in the unexchanged structures [Fig. 5(a)] while the peaks near 1 eV for Au, Cu, and Li in the exchanged structures [Fig. 5(b)]. The Au and the Cu adatoms on the ST site have peaks at about 0.8 eV and 0.9 eV [indicated by Ad in Fig. 5(a)], respectively, and the Ag atoms on the ST site have peaks at ~1 eV [indicated by 4 in Fig. 5(b)]. These peaks are originated mainly from their valence *s* states. On the other hand, the Li adatom on the ST site as well as the Ag atoms at the triangle corners of the Ag layer does not show such a characteristic peak. Thus, the peaks around 0.8–1 eV are the signatures of the *noble atoms* on the *triangle* sites (the similar peaks are also seen in the LT sites), which suggest that the STS spectra can be useful in discriminating the unexchanged and exchanged structures. For alkali metals, if STS spectra taken from the centers of bright features (called "stars") have noticeable peaks different from those of other atoms, they are due to the Ag atoms, implying the exchanged structures. If no peaks are seen in the spectra of stars, the alkali metals occupy the ST or LT sites, i.e., unexchanged structures. For noble-metal adatoms, the peaks will be observed around 0.8–1 eV both in unexchanged and exchanged structures. But the peak positions are slightly different according to the kinds of the adatoms: about 1 eV, 0.8

eV, and 0.9 eV for Ag, Au, and Cu, respectively. Furthermore, in the case of the Au adatom, the peak feature due to Au at a corner of ST, though shifted to a higher energy position, persists even in the exchanged structure [indicated by Ad in Fig. 5(b)] unlike those of usual Ag atoms at the corners of the triangles. Therefore, the calculated site-projected DOSs provide an unambiguous way of verifying an exchanged configuration formed via the exchange mechanism. Indeed, the chemical components of metal chains on a Pd(110) surface have been identified in a recent STS measurement.[29]

IV. CONCLUSION

In conclusion, we explored the diffusions of monovalent metal adatoms (Ag, Au, Cu, Li, Na, and K) on a $\sqrt{3}$-Ag substrate using a first-principles total-energy calculation method. For homogeneous adsorption, diffusion takes place through the exchange of the adatom with substrate atoms. The preference of exchange diffusion over direct diffusion is a consequence of the expanded Ag overlayer. The exchange mechanism leads to the mixing of heterogeneous adatoms (Au, Cu, Li, and Na) with substrate Ag atoms. In contrast, a K adatom favors a direct hopping pathway between metastable sites. This variation in surface diffusion according to adatom has been argued to result from surface stress and adsorption surface chemistry. Calculation of the site-projected DOS provides an unambiguous way of verifying the exchanged diffusion. The calculated results offer a sound microscopic framework for understanding the effects of impurities in the model 2DEG system with the 2DAG on semiconductor surfaces.

ACKNOWLEDGMENTS

This work was supported by a National Research Foundation of Korea Grant funded by the Korean Government (Grant No. KRF-2007-521-C00075).

*jsm@chonbuk.ac.kr

[1] S. Hasegawa, X. Tong, S. Takeda, N. Sato, and T. Nagao, Prog. Surf. Sci. **60**, 89 (1999).
[2] X. Tong, S. Ohuchi, N. Sato, T. Tanikawa, T. Nagao, I. Matsuda, Y. Aoyagi, and S. Hasegawa, Phys. Rev. B **64**, 205316 (2001).
[3] C. Liu, I. Matsuda, R. Hobara, and S. Hasegawa, Phys. Rev. Lett. **96**, 036803 (2006).
[4] J. N. Crain, M. C. Gallagher, J. L. McChesney, M. Bissen, and F. J. Himpsel, Phys. Rev. B **72**, 045312 (2005).
[5] C. Liu, S. Yamazaki, R. Hobara, I. Matsuda, and S. Hasegawa, Phys. Rev. B **71**, 041310(R) (2005).
[6] H. Aizawa and M. Tsukada, Phys. Rev. B **59**, 10923 (1999).
[7] Y. G. Ding, C. T. Chan, and K. M. Ho, Phys. Rev. Lett. **67**, 1454 (1991).
[8] K. J. Wan, X. F. Lin, and J. Nogami, Phys. Rev. B **47**, 13700 (1993).
[9] X. Tong, S. Hasegawa, and S. Ino, Phys. Rev. B **55**, 1310 (1997).
[10] A. Ichimiya, H. Nomura, Y. Horio, T. Sato, T. Sueyoshi, and M. Iwatsuki, Surf. Rev. Lett. **1**, 1 (1994).
[11] J. Nogami, K. J. Wan, and X. F. Lin, Surf. Sci. **306**, 81 (1994).
[12] X. Tong, Y. Sugiura, T. Nagao, M. Takami, S. Takeda, S. Ino, and S. Hasegawa, Surf. Sci. **408**, 146 (1998).
[13] M. Ono, Y. Nishigata, T. Nishio, T. Eguchi, and Y. Hasegawa, Phys. Rev. Lett. **96**, 016801 (2006).
[14] N. Sato, T. Nagao, and S. Hasegawa, Phys. Rev. B **60**, 16083 (1999).
[15] H. Jeong, H. W. Yeom, and S. Jeong, Phys. Rev. B **76**, 085423 (2007).
[16] H. Jeong, H. W. Yeom, and S. Jeong, Phys. Rev. B **77**, 235425 (2008).
[17] M. D'angelo, M. Konishi, I. Matsuda, C. Liu, S. Hasegawa, T. Okuda, T. Kinoshita, Surf. Sci. **590**, 162 (2005).
[18] H. Aizawa, M. Tsukada, N. Sato, and S. Hasegawa, Surf. Sci. **429**, L509 (1999).
[19] G. Kresse and J. Hafner, Phys. Rev. B **47**, 558 (1993); G. Kresse and J. Furthmüller, *ibid.* **54**, 11169 (1996).
[20] D. Vanderbilt, Phys. Rev. B **41**, 7892 (1990).
[21] J. P. Perdew, in *Electronic Structure of Solids '91*, edited by P. Ziesche and H. Eschrig (Academie Verlag, Berlin, 1991).
[22] H. Jeong and S. Jeong, Phys. Rev. B **71**, 035310 (2005); **73**, 125343 (2006).
[23] G. Mills, H. Jonsson, and G. K. Schenter, Surf. Sci. **324**, 305 (1995).
[24] S. Jeong, Surf. Sci. **530**, 155 (2003).
[25] In the exchange processes the energy difference between its initial and final structures are close to the energy barrier because the potential-energy surface near the higher-energy structure is very shallow as seen in Fig. 2(c).
[26] B. D. Yu and M. Scheffler, Phys. Rev. B **56**, R15569 (1997).
[27] J. Tersoff and D. R. Hamann, Phys. Rev. Lett. **50**, 1998 (1983).
[28] W. Humphrey, A. Dalke, and K. Schulten, J. Mol. Graphics **14**, 33 (1996).
[29] D. H. Wei, C. L. Gao, Kh. Zakeri, and M. Przybylski, Phys. Rev. Lett. **103**, 225504 (2009).